

Experimental investigation on the shear capacity of RC dapped end beams and design recommendations

Quanfeng Wang[†] and Zixiong Guo[‡]

College of Civil Engineering, Huaqiao University, 362011 Quanzhou, Fujian, China

Pierre C.J. Hoogenboom[‡]

Department of Civil Engineering, Delft University of Technology, 2600 GA Delft, Netherlands

(Received January 19, 2004, Accepted June 24, 2005)

Abstract. In this paper, the shear resistance behaviour of reinforced concrete (RC) dapped end beams is investigated by 24 tests until failure load. The main parameters considered are the dapped end height, the type and effective range to provided the stirrups and the bent form of the longitudinal reinforcement. The failure behaviour of dapped end beams is presented and some conclusions are given. Inclined stirrups and longitudinal bent reinforcement have more influence on the shear capacity than vertical stirrups. Additionally, the shear mechanism of dapped end beams is analysed. Relatively simple semi-empirical equations for shear strength have been derived based on the results of 22 dapped end beams. The predicted results are in close agreement with the experimental ones. Finally, some design suggestions for the ultimate shear strength of dapped end beams are presented.

Key words: reinforced concrete (RC); dapped end beams; shear capacity; shear failure; ultimate shear strength; shear resistance mechanisms.

1. Introduction

The extensive study of the behaviour of reinforced concrete flexural members has clarified the flexural behaviour mechanism to the extent that well-understood conclusions are now incorporated in the design codes of many countries. Progress in the understanding and quantitative assessment of the behaviour of members subjected to flexure and shear have been somewhat less spectacular. The majority of structural members in RC must resist shear forces. These forces seldom act on their own but rather in combination with flexural, axial load, and perhaps torsion. The problem of how shear failures occur in RC still remains, despite numerous extensive studies over the last 50 years (Zararis *et al.* 2001, Leonhardt *et al.* 1984, Schlaich *et al.* 1987, Thomas 1998). Because of these complexities, codified methods continue to include expressions for shear resistance based on fitting curves to experimental data. Strong evidence of this is the fact that international codes, such as the code of the American Concrete Institute (ACI) (1999) or the Eurocode 2 (1992) are based on rather

[†] Professor, Corresponding author, E-mail: qfwang@hqu.edu.cn

[‡] Associate Professor

(semi-) empirical considerations (Zararis *et al.* 2001). Unfortunately, empirical results cannot be correctly extrapolated to beams of more complicated shape such as RC dapped end beams. In the international design community for structural concrete a distinction between B-regions and D-regions is used. B-regions are the parts of a structure in which the classic beam theory applies. The remaining part of the structure consists of D-regions in which the fore-mentioned classic state is disturbed. Examples are joints between beams and columns, zones around holes in the web of a beam, deep beams, corbels, brackets, shear walls having an irregular shape (Blaauwendraad *et al.* 2000). A short beam having dapped ends would be considered as one D-region. RC dapped end beams differ from general flexural members in that transfer of shear force may be of more critical importance. In a dapped end beam, where inclined cracking under combined stress states occurs, a significant redistribution of internal forces can be expected after cracking, and a large part of the shear force is transferred by what is known as the truss mechanism (Leonhardt *et al.* 1984, Schlaich *et al.* 1987, Thomas 1998). In addition to identifying the effect of shear forces acting alone, it is necessary to examine the possible interaction with other structural actions. In flexural members in particular, the shear resisting mechanisms interact intimately with the bond between concrete and the embedded reinforcement of the latter. Though extensive experimental work, particularly in recent years, has greatly extended the identification of various shear resistance mechanisms (Zararis *et al.* 2001), very few tests on RC dapped end beams have been performed. Up to present, only a total of 38 dapped end beam tests were report in literal by Mattock *et al.* (Mottaock *et al.* 1979, Mottaock 1986), which included both RC and prestressed concrete dapped end beam. The present paper reports the test results of 24 RC dapped end beams. For these beams, the effects of the dapped end height, the type and effective range to provide the stirrups, and the bent form of the longitudinal reinforcement on the shear capacity were studied in detail.

2. Research significance

This study adds test data of 24 RC dapped end beams to a field in which few test studies have been performed and thus has theoretical and practical significance. The failure behaviour of dapped end beams is presented, and some design suggestions, as well as a series of semi-empirical equations for shear strength are given. These results are valuable references for engineers who are confronted with the design of RC dapped end beams and other shear dominated components.

3. Experimental program

Shear transfer in reinforced concrete dapped end beams, as well as in general reinforced concrete beams, relies heavily on the tensile and compression strength of the concrete. Thus it is not surprising that a shear failure in general is non-ductile. In practice, flexural failure could occur before shear failure. However, for these experiments the shear failure must occur prior to any other type of failure such as bond, flexure, splitting etc. This implies that the maximum flexural strength of the beam must be somewhat in excess of the shear strength it could possibly develop. In the test program, 22 of the 24 specimens collapsed after arriving at the shear capacity. The collapse of 2 specimens (B1.21 and B2.32) resulted from the compression crushed of the cracked reinforced concrete and splitting failure of concrete, respectively.

3.1 Test specimens

Three series, B1, B2 and B3 of RC dapped end beams were tested. The overall dimensions of each series are shown in Fig. 1. All tested beams had the same length of 1500 mm. The location of centre lines of loads and supports were the same for all test specimens. The details of reinforcement and the sizes for each beam are shown in Fig. 1 and Table 1.

The specimens range from I to III. In Table 2, the specimen number $Bk.ij$, subscript k is the number of the beam series 1, 2, 3; subscript i is the number of the beam and subscript $j = 1$ or 2, which denote the first or second end of the beam, respectively.

In Table 1 f_{cu} is the compressive strength of standard cube ($150 \times 150 \times 150$); f_c is the cylinder compressive strength; b and h are the width and depth of the dapped end beam as shown in Fig. 1, respectively; h_1 and h_{10} are the height and the effective height of the dapped end, respectively; λ is the shear span/depth ratio of the dapped end beam; a is the distance from the load applied point to the support as shown in Fig. 2; $1\Phi 6$ means a 6 mm diameter vertical stirrup with 2 legs; and $1\Phi 14 (45^\circ)$ means one 14 mm diameter normal mild bar bent along 45° ; a_1 is the distance of the first stirrup to the end face of dapped end beam; and a_0 is the effective range of stirrups.

Table 1 Specimen details and failure loads V_u^T

Series	No.	Concrete Strength MPa		Dimensions (mm)				$\lambda = a/h_{10}$	Web Reinforcement Provided	Range of Stirrups mm		Failure Load V_u^T (kN)
		f_{cu}	f_c	b	h	h_1	h_{10}			a_1	a_0	
I	B1.11	16.90	11.32	214	370	170	145	3.38	1Φ8+1Φ14 (90°)	50	50	58.77
	B1.12	16.90	11.32	214	370	164	139	3.23	1Φ6	60	60	42.24
	B1.21	16.01	10.73	220	370	190	165	2.83	1Φ8+1Φ18 (45°)	105	105	65.00
	B1.22	16.01	10.73	220	370	160	135	3.13	2Φ8@42	45	87	72.98
II	B2.11	19.53	13.09	150	300	150	125	2.0	1Φ6	30	30	34.75
	B2.12	19.53	13.09	150	300	150	125	2.0	1Φ6	100	100	31.75
	B2.21	19.53	13.09	150	300	150	125	2.0	2Φ6@70	30	100	55.22
	B2.22	19.53	13.09	150	300	150	125	1.9	2Φ6@64	40	104	65.83
	B2.31	19.53	13.09	150	300	150	125	1.87	1Φ6+1Φ14 (45°)	40	40	75.73
	B2.32	19.53	13.09	150	300	150	125	2.0	1Φ6+1Φ14 (45°)	75	75	65.0
III	B3.11	25.89	18.12	150	315	160	130	2.31	2Φ6@30	30	60	60.0
	B3.12	25.89	18.12	150	315	160	130	2.31	2Φ6@30	22	52	70.0
	B3.21	25.89	18.12	150	300	150	120	2.50	2Φ6@35	25	60	66.0
	B3.22	25.89	18.12	150	300	150	120	2.50	2Φ6@30	45	75	50.0
	B3.31	22.82	15.97	150	305	150	120	2.50	1Φ6 with 4 legs	50	50	52.2
	B3.32	22.82	15.97	150	305	150	120	2.50	2Φ6@45 with 4 legs	20	65	63.0
	B3.41	22.82	15.97	150	310	100	75	4.07	1Φ6@35	30	30	26.8
	B3.42	22.82	15.97	150	310	100	75	4.0	1Φ6@35	40	40	26.4
	B3.51	22.82	15.97	150	305	155	125	2.4	1Φ6+1Φ14 (45°)	30	30	79.1
	B3.52	22.82	15.97	150	305	150	120	2.5	1Φ6+1Φ14 (45°)	30	30	75.0
	B3.61	22.67	15.19	150	300	150	128	2.34	2Φ6+1Φ14 (90°)	38	68	63.2
	B3.62	22.67	15.19	150	300	150	128	2.42	2Φ6+1Φ8 with slop legs	23	58	92.8
	B3.71	22.67	15.19	150	300	150	128	2.34	2Φ6+1Φ8 (45°)	23	58	90.0
	B3.72	22.67	15.19	150	300	150	128	2.38	2Φ6+2Φ8 (45°)	13	56	116.2

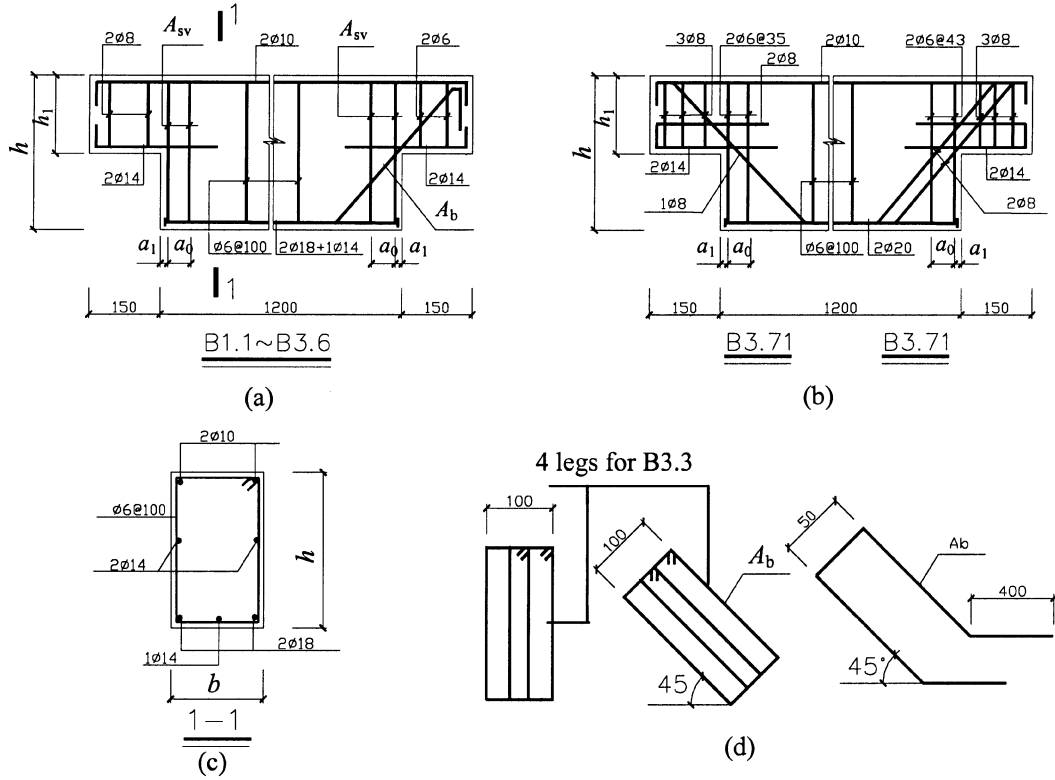


Fig. 1 Specimen geometry and reinforcement detailing

The form and the amount of web reinforcement included three levels: a low amount, a large amount, and with the longitudinal bar bent and inclined at an angle of 45° to the horizontal. For Series II, called B2.*ij*, these were varied to obtain six different dapped end beams as shown in Fig. 1(a). For Series I and III, called B1.*ij* or B3.*ij*, in addition, the height of the dapped end was varied to obtain different shear span-to-depth ratios as shown in Figs. 1(a), (b). The difference between Series I and III is the form of web reinforcement including the inclined stirrup, the stirrup with 4 legs and f_c . The longitudinal reinforcement was kept constant for each series except for the beams in Series III (B3.7), where the amount of the reinforcement was increased. All main longitudinal reinforcements extended over the full length of the beams bottom and were welded on steel plates embedded at the ends of the beams to provide sufficient anchorage (Fig. 1).

3.2 Material

The constituents of the concrete were ordinary Portland cement, irregular gravel of 10 mm maximum size, and sand. The mix proportions by weight are given in Table 2 for the beams in Series I and II, and in Table 3 for the beams in Series III.

All specimens were cast in wooden formwork and specially differed in the dapped end height and the overall depth. The following control specimens were made during casting of each beam: three $150 \times 150 \times 150 \text{ mm}^3$ cubes for beams in every series. The cubes were tested on the same day of

Table 2 Concrete constituents for beams in Series I and II

Ingredients	Weight (kN/m ³)	Weight/Cement content
Water	1.95	0.62
Cement	3.15	1.00
Sand	6.57	2.09
Gravel	11.19	3.55

Table 3 Concrete constituents for beams in Series III

Ingredients	Weight (kN/m ³)	Weight/Cement content
Water	1.80	0.46
Cement	3.90	1.00
Sand	6.29	1.61
Gravel	12.00	3.08

the beam test. The cube compressive strength f_{cu} shown in Table 1 was obtained from the average of the compressive strengths of the tested cubes. The applied relation between the cube compressive strength f_{cu} and cylinder compressive strength f_c is

$$f_c = 0.67f_{cu}$$

All reinforcing bars were rolled out of normal mild steel. The yield stress f_y was obtained by tension tests.

3.3 Instrumentation

The specimens were heavily instrumented to obtain as much information as possible. Most of the results was recorded automatically using the data logger and the rest was measured manually. The load cell reading was recorded automatically using the data logger. Steel strains were measured using 5×3 mm electrical resistance strain gauges (ERS). All ERS gauges used in one beam were concentrated on one end of the dapped end beam. The number of ERS gauges used was varied from one end to another end depending on the amount of the web reinforcement. The concrete strains were measured across 100 mm² gage length demic points. The midspan deflection of each beam was measured using a demountable mechanical strain gauge with 10 mm capacity.

3.4 Test setup

The test specimens were subjected to four-point-bending in a compression machine with a total capacity of 500 kN. A top steel spreader beam was used to divide the total applied load from the machine head into two equal point loads as shown in Fig. 2. The load was applied in increments of 10 kN until failure occurred. After each increment, the load was kept constant to allow marking of the new cracks and running of the data logger. The test was under load control until the specimen reached its peak strength.

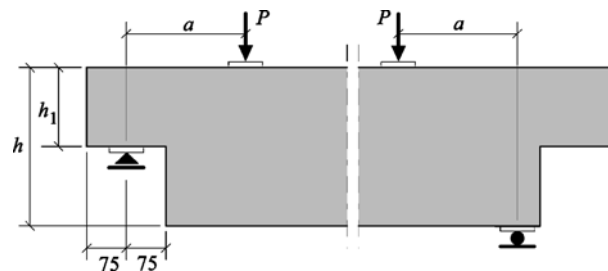


Fig. 2 Test set-up

4. Results of tests and analyses

4.1 Crack formation and shear failure modes

The typical crack pattern and failure modes of these dapped end beams reported in this paper are shown in Fig. 3. In the tests, cracks always initiated at the reentrant corner of the dapped end beam at approximate 40° - 60° to the axis of the beam, resulting in a redistribution of stresses causing increasing steel stresses, bond stresses and some bond slip. Under an additional load these cracks spread, increased in number and reduced the compression zone of the beam considerably. At one or a few load increments before failure, more inclined cracks (about 3), occurred at the reentrant corner of the majority of dapped end beams, and steeper (50° - 70°) than the first inclined crack up to

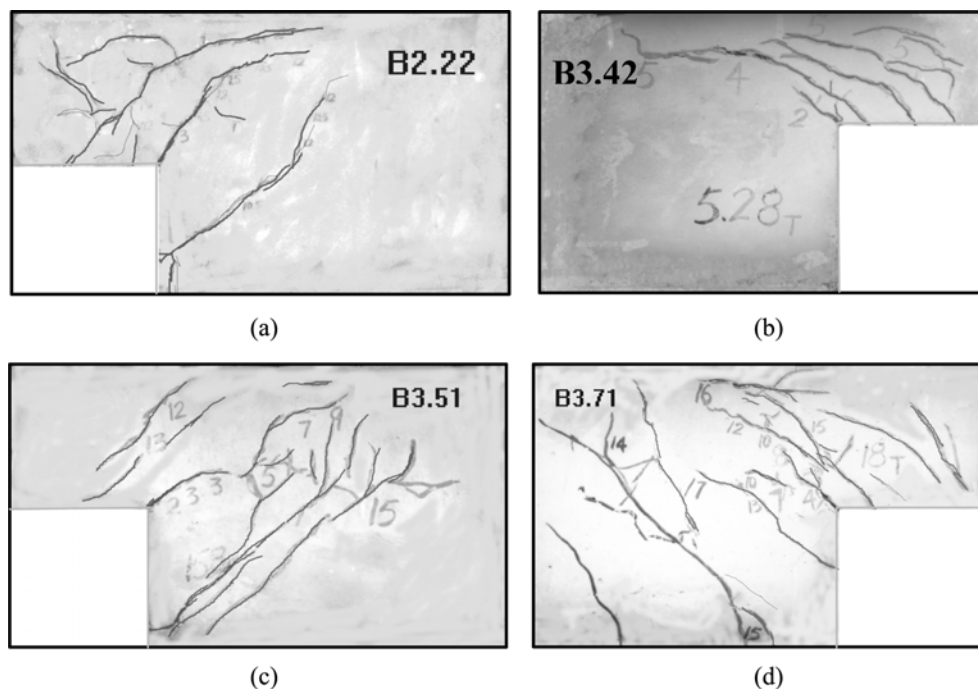


Fig. 3 Failure modes

the vicinity of the load point. A critical inclined crack occurred suddenly, which activated resistance to stresses in the web reinforcement, aggregate interlock along the diagonal crack, if any exists, as well as resistance in the uncracked concrete above the head of the crack. Under the increasing load, the diagonal crack propagated towards the loading point causing an increase in the dowel shear, and final failure occurred when the head of the diagonal crack had decreased the uncracked compression block of concrete to a critical point at which time a so-called “shear-compression” failure occurred under a combined state of stress. As the reinforcement was yielding, cracks became wide and the deflection significantly increased. When the cracks had developed to some extent, the tension in the web reinforcement at the vicinity of the reentrant corner increased as the inclined cracks gradually developed.

A majority of the beams developed some cracks at the bottom edge before reaching their ultimate failure due to redistribution of internal forces (See Figs. 3c and 3d). Exceptions were B2.22 which had more web reinforcements, and B3.42 which had the smallest nib height (See Figs. 3a and 3b).

The tests show that the first inclined crack initiated at 13-45% of the failure load. Such inclined cracks, known as diagonal tension cracks, were generally controlled adequately by the shear reinforcement. The results indicate that the height of the cross section of the specimens played an important part in the crack control. The effect of web reinforcement on the control of diagonal tension cracks was not significant compared to the dimension of cross section.

The specimen B3.72, which had detailed with two vertical and two inclined stirrups, showed the largest failure load, whereas the specimen B1.21 detailed with a similar amount of web reinforcement to specimen B3.72 had relatively lower shear strength than that of B3.72. This is because that the above two specimens have a rather different failure mechanism. The specimen B3.72 reached its ultimate shear strength after its web reinforcement yielded, whereas the concrete of specimen B1.21 was crushed before the web reinforcement yielded for its relatively low concrete strength (f_c is only 10.73 MPa).

The crack pattern and failure mode of specimen B3.41 and B3.42 were clearly different from other specimens (See Fig. 3b). The inclined cracks are concentrated above the support platen of the nib and no crack can be seen under the reentrant corner. Noted that the nib depth of B3.41 and B3.42 are only $0.33 h$ and their shear span to depth ratio is up to 4.0. This result in its resistant mechanism is rather different compared to that of other specimens (Fig. 7). The internal arching effect of B3.41 and B3.42 is weakened for their large shear span to depth ratio, and thus showed relative low shear strength.

4.2 Strains of reinforcement and concrete

In some cases, the electrical resistance strain (ERS) gauges were near but not at major crack positions, and so yielding has occurred at the crack even though this was not shown by the ERS gauges. In the following the variation of strains in several reinforcing bars against the total applied load is presented for B3.32. B3.32 had vertical stirrups with 4 legs as shown in Fig. 1(c). Fig. 4(a) shows the positions of different ERS gauges attached to the stirrups at approximately 45° to the axis of the beam. Fig. 5 presents the variation of steel strains of different bars and positions with the total applied load. The longitudinal reinforcement 103 yielded first. The vertical stirrup with 4 legs near the dapped end was very close to yielding. Just before failure, major redistribution of the vertical stirrup strain took place and stirrup 102 yielded.

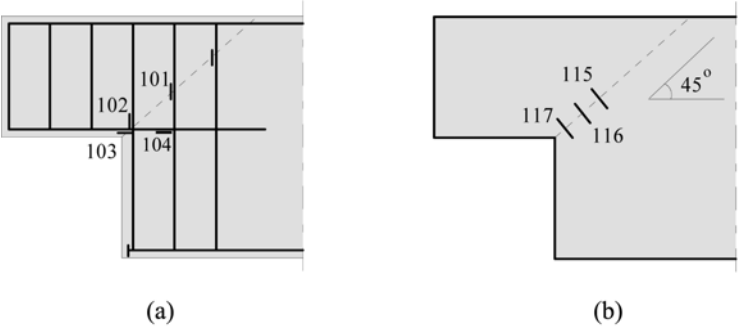


Fig. 4 Positions of the strain gauges

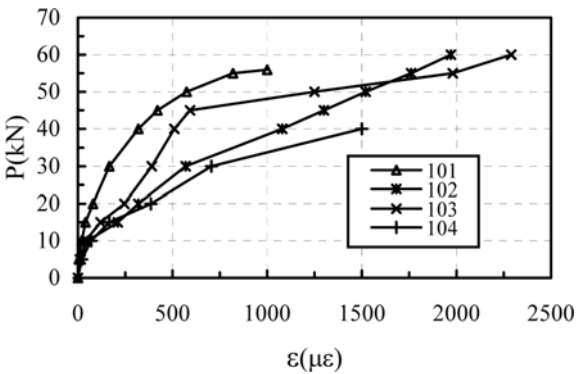


Fig. 5 Shear-strain curve for B3.32 reinforcement

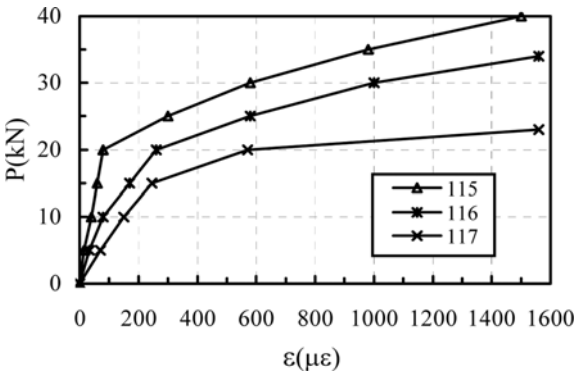


Fig. 6 Shear-strain curves for B3.51 concrete

Fig. 4(b) shows the positions of some of the ERS gauges attached to the concrete surface at approximately 45° to the axis of the beam. Fig. 6 presents the strains recorded on the concrete surface at the beginning of loading for beam B3.51. The strain of the concrete increased as the loading increased, and the largest strain occurred at the vicinity of the reentrant corner. Along the inclined crack the values of the strains decreased.

4.3 Effect of stirrup variation on shear capacity

The reinforcement details for each specimen are shown in Fig. 1 and Table 1. In the test, 14 specimens were provided with vertical stirrups or closed stirrups. Only two of these specimens had stirrup with 4 legs; three specimens were provided with vertical stirrups and inclined stirrups, and 10 specimens had vertical stirrups and bent longitudinal reinforcement. By comparing the shear capacity of specimens with vertical stirrups (B3.11-B3.22) to specimens with inclined stirrups (B3.62, B3.71 and B3.72), it can be concluded that the inclined stirrups had more influence on the capacity than the vertical stirrups had. The reason is that when inclined reinforcement crosses a crack subjected to shear displacements, a significant part of the shear force may be transferred by dowel action in these bars. From the tests, it also can be seen that closed stirrups will enhance the shear resistance capacity, but less than the inclined stirrups and the bent reinforcement.

4.4 Effect of the bent form of longitudinal reinforcement on shear capacity

The shear capacities of specimens B1.11 and B3.61 are given in Table 1. B1.11 and B3.61 with combined vertical stirrups and web bar bent along 90° had a smaller shear capacity than B1.21 and B3.52 with combined vertical stirrups and web bars bent along 45°. Therefore, it is recommended not to use the bent form along 90° of the longitudinal reinforcement.

Table 4 Comparisons of predicted shear strength and experimental shear strength

No.	$f_c b h_{10}$ kN	$A_{sv} f_{yv}$ kN	$A_{sb} f_y \sin \alpha$ kN	V_u^T kN	V_u^c kN	$V_u^{c'}$ kN	V_u^c / V_u^T	$V_u^{c'} / V_u^c$
B1.12	336.72	24.42		42.24	39.34	95.32	0.931	2.423
B1.21*	389.50	33.60	61.94	65.00	112.05	81.35	1.724	0.726
B1.22	318.68	67.05		72.98	74.95	99.84	1.027	1.332
B2.11	245.44	24.42		34.75	34.36	105.65	0.989	3.075
B2.12	245.44	24.42		31.75	34.36	63.39	1.082	1.845
B2.21	245.44	48.84		55.22	55.32	105.65	1.002	1.910
B2.22	245.44	48.84		65.83	55.32	96.46	0.840	1.744
B2.31	245.44	24.42	37.47	75.73	71.83	96.46	0.949	1.343
B2.32**	245.44	24.42	37.47	65.00	71.83	73.95	1.105	1.030
B3.11	353.34	54.0		60.00	65.64	109.88	1.094	1.674
B3.12	353.34	67.0		70.00	76.80	118.94	1.097	1.549
B3.21	326.16	54.0		66.00	64.16	106.49	0.972	1.660
B3.22	326.16	54.0		50.00	64.16	88.75	1.283	1.383
B3.51	299.44	27.0	37.45	79.10	76.97	105.65	0.973	1.373
B3.52	299.44	27.0	37.45	75.00	76.97	101.42	1.026	1.318
B3.62	291.65	53.9	23.80	92.80	85.99	115.91	0.927	1.348
B3.71	291.65	53.9	23.80	90.00	85.99	115.91	0.955	1.348
B3.72	291.65	53.9	47.60	116.20	109.79	129.08	0.945	1.176

Note: V_u^c is the calculated shear strength from Eq. (9); $V_u^{c'}$ is the calculated shear strength from Eq. (11); V_u^T is the experimental shear strength.

* -- the compression crushed of the cracked reinforced concrete;

** -- the splitting failure of the concrete.

4.5 Effect of nib depth on shear capacity

In addition to the various stirrups provided, variables of importance to the shear capacity included the depth of the dapped end and the effective range of the stirrups. The shear capacities of specimens B1.12, B2.11 and B2.12 are given in Table 1. B1.12 had a higher dapped end than B2.11 and B2.12. We can see that B1.12 had the same reinforcement as B2.11 and B2.12 in Table 4, the test data showed that B1.12 had larger shear capacity than B2.11 and B2.12, although the later had larger compressive strength f_c' . The same can be seen from the comparison between B3.4 and B1.12 or B2.11. B3.41 and B3.42 had a dapped end height of $0.33 h$ and showed a very small shear strength. The effect of the dapped end height on shear capacity is significant. From the tests it is recommended that the dapped end height should not be less than $0.45 h$ (Mottaock *et al.* 1979).

4.6 Effective range of beam where stirrups are provided

The distance, a_1 of the first stirrup from the end face of dapped end beam and the length, a_0 where stirrups are provided (Fig. 7), affected the shear capacity of the dapped end beams. The conditions of B2.11 and B2.12 were the same except that specimen B2.11 had a smaller value of a_1 , whereas B2.11 showed a larger shear capacity than B2.12. The same can be seen in the second group from the comparison between B3.21 and B3.22. Therefore the effect of the distance, a_1 of the first stirrup from the end face of the dapped end beam cannot be ignored. To obtaining this value, the concrete covers of all first stirrups were removed after testing. The measured distance, a_1 was between 15 mm (prescribed concrete cover of stirrup) and 40 mm. The strains in the stirrups decreased as the distance from the end face of dapped end beam increased. Note that not all the stirrups provided in a_0 could contribute themselves to the shear capacity of the dapped end beams. In this paper, the length a_0 in which the stirrups could effectively contribute to the shear capacity are referred to as effective range. By analysing the variation of strains of the stirrups and directly measuring the spacing of the stirrups, the effective range to provided the stirrups is recommended to be $a_0 = 0.5 h_1$ (Wang *et al.* 1996).

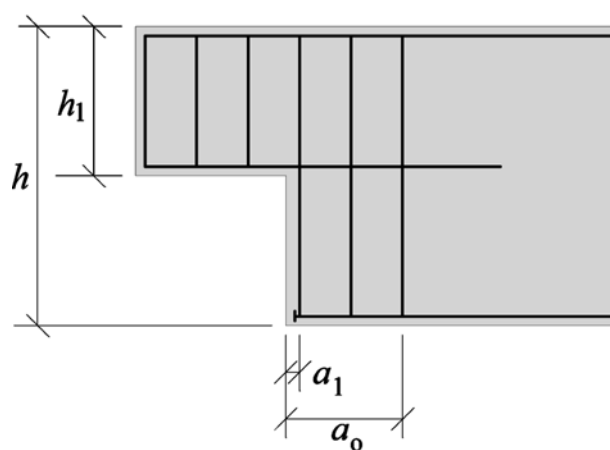


Fig. 7 The position of a_1 and a_0

5. Mechanism of shear resistance and design for shear

5.1 Truss mechanism

5.1.1 Vertical stirrups provided only

The analogous truss shown in Fig. 8(a) depicts the case of orthogonal reinforcement. In Fig. 8, T denoted tension (solid line) and D denoted compression (dashed line). It will serve to illustrate the relation between external shear forces V_s , to be resisted by the truss, and the various internal forces. The forces in the truss can be determined from considerations of equilibrium only:

$$V_s = T_s \quad (1)$$

$$T_1 = V_s \times \frac{e}{Z_1} \quad (2)$$

in which T_s is the resultant of all stirrup forces within the effective range a_o ; T_1 is the resultant in the flexural reinforcement at the end of the dapped end beam; e is the distance from the centre of the support to T_1 and Z_1 is the distance from T_1 to the centre of D .

5.1.2 Inclined web reinforcement only

The analogous truss shown in Fig. 8(b) depicts the general case of web reinforcement inclined at an angle α to the horizontal. It will serve to illustrate the relation between external shear forces V_s , to be resisted by the truss, and the various internal forces. The forces in the truss can be determined from considerations of equilibrium only:

$$V_b = D_1 \quad (3)$$

$$D_1 = T_{sb} \times \sin \alpha \quad (4)$$

and

$$T_{sb} = A_{sb} \times f_y$$

$$V_b = A_{sb} \times f_y \times \sin \alpha \quad (4a)$$

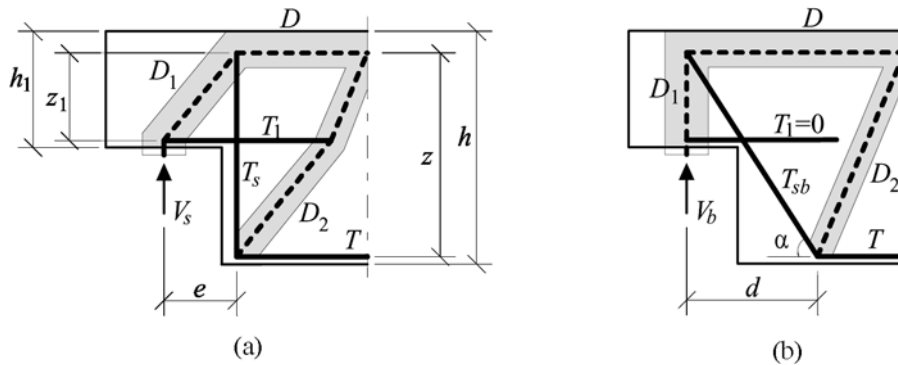


Fig. 8 Internal forces in analogous trusses of the dapped end beam

In which V_b is the bearing capacity of dapped end beam when the inclined web reinforcement was provided; T_{sb} is the resultant of all inclined web reinforcements provided; A_{sb} is the area of the inclined web reinforcement, and f_y is the stirrup stress.

5.2 Design for shear of the dapped end beam

After cracking, substantial redistribution of internal forces occurred. For the dapped end beam, the total shear resistance V_N in a typical region is comprised of the sum of that of the still uncracked portion of the concrete section and interface shear transfer V_c across the crack by aggregate interlock and the force V_s transferred by direct tension in the stirrup

$$V_N = V_c + V_s \quad (5)$$

If the vertical stirrups and the inclined web reinforcement are combined, the following equation results

$$V_N = V_c + V_s + V_b \quad (6)$$

5.2.1 Vertical stirrups only

The shear resisting mechanism of a beam without web reinforcement, relying only on aggregate interlock action, will function as long as the width of the cracks does not become excessive. The interface shear transfer can be expressed as

$$V_c = \beta_1 \times f_c \times b \times h_{10}$$

In which β_1 is a coefficient to be determined by regression analysis of the test results. None of the stirrups yielded within their effective range according to the test results in Table 2. Hence in the presence of stirrups, we use

$$V_s = \beta_2 \times A_{sv} \times f_{yv}$$

In which β_2 is also a coefficient to be determined by regression analysis of the test results; A_{sv} is the total cross section area of the vertical stirrups within the effective range. Substituting the above equations into Eq. (5) gives

$$V_N = \beta_1 \times f_c \times b \times h_{10} + \beta_2 \times A_{sv} \times f_{yv} \quad (7)$$

5.2.2 Combined vertical stirrups and inclined web reinforcement

When vertical stirrups and inclined web reinforcement are combined, besides the shear resisted partly by the vertical stirrup V_s and partly by the previously described concrete struts V_c , the third term of Eq. (6) signifies that the shear was sustained by the inclined web reinforcement as expressed by Eq. (4a)

$$V_b = \beta_3 \times A_{sb} \times f_y \times \sin \alpha$$

Measurements on the dapped end beam indicated that the shear strength with inclined web

reinforcement was higher than the shear strength with vertical stirrups, but was the same as the shear strength with the longitudinal reinforcing bent at an angle of 45° . By taking $\beta_3 = 1.0$, Eq. (6) can be expressed as

$$V_N = \beta_1 \times f_c \times b \times h_{10} + \beta_2 \times A_{sv} \times f_{yv} + A_{sb} \times f_y \times \sin \alpha \quad (8)$$

Thus far, it had not been possible to rationally allow for all factors affecting each of the components of the shear resisting mechanisms and their interaction. By using statistical regression analysis of the test results of 16 specimens (without B1.21 and B2.32 as shown in Table 4), the two most important parameters governing shear strength were derived: $\beta_1 = 0.0546$ and $\beta_2 = 0.8583$. So, the following equation to account for the shear strength of dapped ends beam is proposed

$$V_N = 0.0546 \times f_c \times b \times h_{10} + 0.8583 \times A_{sv} \times f_{yv} + A_{sb} \times f_y \times \sin \alpha \quad (9)$$

5.3 Demand of longitudinal reinforcement at the nib of the dapped end beam

If only vertical stirrups are provided, by approximately taking $Z_1 = 0.85 h_{10}$, Eq. (2) becomes

$$T_1 = 1.18 \frac{e}{h_{10}} \cdot V_u \quad (10)$$

The minimum amount of longitudinal reinforcement in the nib of a dapped end beam can be determined from the above equation.

If the shear strength of a dapped end beam is controlled by the flexural strength of its nib, the shear strength can also be determined by Eq. (10) and can be expressed as follows

$$V_N = \frac{A_{s1} \cdot f_y \cdot h_{10}}{1.18e} \quad (11)$$

In which A_{s1} is the area of longitudinal reinforcement detailed at the nib of a dapped end beam; f_y is the yield stress of longitudinal reinforcement; h_{10} is the effective high of nib and e is the shear span defined in Fig. 8.

6. Comparison of results

The predicted shear strength of the dapped end beams can be determined by smallest value of shear strength calculated by Eq. (9) and Eq. (11). Table 4 shows the comparison of calculation results and test results of 18 specimens. The other 6 specimens exist of exception, and thus are excluded from comparisons. Exceptions are B3.31 and B3.32, having the stirrups with 4 legs, B3.41 and B3.42 with the smallest dapped end height (less than $0.45 h$), B1.11 and B3.61 with vertical stirrups combined with web bar bent along 90° .

It is noted that the values calculated by Eq. (9) are larger than that by Eq. (11) for all specimens but specimen B1.21 due to adequate amount of longitudinal reinforcement in the nib.

Table 4 shows a good agreement between test and calculation results for most specimens except that the result of specimen B1.21 showed large scatter between calculation and test result. It should be noted that the specimen B1.21 was provided with a largest web reinforcement and smallest

concrete strength than that of other specimens, and thus resulted in a compression failure before the web reinforcement arriving its yield stress.

7. Conclusions

From the tests the following behavior was observed and some design recommendations are given:

- (a) 22 test specimens collapsed after arriving at the ultimate load due to loss of their shear capacity. Exceptions are specimen B1.21 and specimen B2.32 in which collapse resulted from the compression crushed of the cracked reinforced concrete and splitting failure of concrete, respectively. The first crack always initiated at the reentrant corner of the dapped end beam at approximately 40° - 60° to the axis of the beam. Obviously, the cracks developed as the load increased.
- (b) The inclined cracks, up to the vicinity of the load point, occurred at the reentrant corner of the dent. Under increasing load, the diagonal crack propagated towards the loading point and final failure occurred when the tip of the diagonal crack decreased the uncracked compression block of concrete to a critical point when a so-called shear-compression failure occurred.
- (c) The cross-sectional dimensions of the specimen played an important role in control of the diagonal cracks, and the effect of the web reinforcement on crack control was not significant, compared with the size of the cross section;
- (d) From the tests, it also can be seen that closed stirrups enhance the shear resisting capacity, but less than inclined stirrups and bent reinforcement.
- (e) The effect of the height of the nib end on shear capacity is significant. It is suggested that the height of the nib end should be larger than $0.45 h$.
- (f) The distance of the first stirrup to the end face of the dapped end beam is recommended to be less than 40 mm and as close to the end face of the dapped end beam as possible. The effective range of the stirrups is proposed to be $a_o = 0.5 h_1$.
- (g) Some relatively simple semi-empirical equations for shear strength are proposed in this paper based on the test results of 16 dapped end beams. The results predicted by these equations are in good agreement with test results presented in this paper. The predicted shear strength by Eq. (9) can be used for different types of web reinforcement.
- (h) The minimum amount of longitudinal reinforcement at the nib of a dapped end beam can be determined from Eq. (10) to prevent the flexural failure of the nib.

Acknowledgements

The work described in this paper was carried out in the Huaqiao University. The assistances of the staff are gratefully acknowledged.

References

American Concrete Institute (ACI) (1999), "Building code requirements for structural concrete and commentary", ACI 318-99, Detroit.

- Blaauwendraad, J. and Hoogenboom, P.C.J. (2000), "Design tool for structural concrete D-regions", *Proc. of the Int. Symp. on Modern Concrete Composites & Infrastructures (MCCI'2000)*, Northern Jiaotong University, Beijing, China, **1**, 3-10.
- European Committee for Standardization (CEN) (1992), "Design of concrete structures, Part 1: General rules and rules for buildings", Eurocode 2, Brussels.
- Leonhardt, F. (1984), *Grundlagen zur Bemessung im Stahlbetonbau (Teil 1, Dritte Auflage)*, Springer-Verlag, UK.
- Mottaock, A.H. and Chan, T.C. (1979), "Design and behavior of dapped end beams", *Prestressed Concrete Institute Journal*, **24**(6), 28-45.
- Mottaock, A.H. (1986), "Behavior and design of dapped end members", *Proceedings, Seminar of Precast Concrete Construction in Seismic Zones*, Tokyo, 81-100.
- Schlaich, J., Schafer, K. and Jnnewein, M. (1987), "Toward a consistent design of structural concrete", *Prestressed Concrete Institute Journal*, **32**(3), 74-150.
- Thomas, T.C. (1998), "Unified approach to shear analysis and design", *J. Cement and Concrete Composites*, **20**, 419-435.
- Wang, Quanfeng, *et al.* (1996), "Study on detailing at the ends of notched concrete beams", *Proc. on Studies and Applications of Joint Connections of Concrete Structures and of Structural Earthquake Resistant Detailing*, 115-121, Qingdao, China (in Chinese).
- Zararis, P.D. and Papadakis, G.C. (2001), "Diagonal shear failure and size effect in RC beams without web reinforcement", *J. Struct. Eng.*, ASCE, **127**(7), 733-742.